Quality and Performance Improvements of Nb Microalloyed Steels Based on Modeling Approaches for TSCR Route

ISASTI N.[1,2], URANGA P.[1,2], RODRIGUEZ-IBABE J. M.[1,2], LV D.W.[3], XI J. T.[3], LIU Z. Z.[4]

(1. CEIT, P. M. Lardizabal 15, 20018, San Sebastian, Basque Country, Spain; 2. Universidad de Navarra, Tecnun, P. M. Lardizabal 13, 20018, San Sebastian, Basque Country, Spain; 3. HBIS Group Hansteel Company, Handan, Hebei, China; 4. CITIC Metal Co., Ltd., Beijing, China)

Abstract: This paper analyzes the application of a proper combination of detailed microstructural analysis and microstructural modeling to achieve a cost-effective processing optimization and accomplishment of the required mechanical properties in Nb microalloyed steel grades. This approach is applied for the TSCR industrial process of Handan steel plant. An extensive microstructural analysis, including conventional and EBSD techniques, was done in several low carbon HSLA steel grades. Once this done, with the help of MicroSim-DSP® model and the process parameters of each selected steel, the austenite grain size distributions were predicted from pass to pass during the overall hot rolling process. This allowed the identification of main metallurgical changes, such as as-cast austenite grain refinement, Nb(C,N) strain induced precipitation and posterior austenite pancaking. Based on microstructural predictions, the mean flow stress evolution was calculated and the resulting values compared with real data measured in the plant. This allowed an evaluation of the precision of the microstructural model. Finally, the most relevant process steps during hot rolling were identified that could allow an additional improvement of the sheet quality.

Key words: Nb microalloyed steels, modelling, microstructure, EBSD

Thin Slab Casting and Direct Rolling (TSCR) routes have achieved a well defined technological position in the flat product field. This near-net-shape technology has several singularities, such as the presence of as-cast microstructure at the entry of the first rolling pass and the limited total reduction during hot rolling. Both singularities affect the metallurgical design of HSLA steels and the definition of the processing parameters. In this context, the development of microstructural models helps in the proper definition of microalloying concept and in the optimization of rolling parameters [1, 2].

Hansteel TSCR production covers a wide range of thicknesses and chemical compositions, including HSLA structural Nb-based microalloyed steels. Based in this industrial application, this paper analyzes, considering laboratory studies and modelling tools, how to optimize Nb based steel grades production. Microstructural characterization of industrial samples was performed using conventional microscopy and EBSD analysis. In addition, MicroSim-DSP® microstructural model was tailored to implement the mill characteristics and adapted as a complementary tool in process design. Finally, with a combined evaluation of microstructural characterization and model predictions, the role of each metallurgical strengthening mechanism is considered.

1 Experimental Techniques

Table 1 summarizes the steel grades selected. They correspond to different microalloyed grades produced by TSCR technology, with final gauge thicknesses ranging from 2 to 5mm. The microstructures were characterized by optical microscopy and FEG-SEM microscopy. Electron Backscattered Diffraction (EBSD) scans were performed to quantify the crystallographic features intervening in the mechanical behavior. For this purpose, the samples were polished to 1μm followed by a finishing with colloidal silica. Orientation imaging microscopy was carried out on the

Philips XL30CP SEM with W-filament, using TSL equipment. The selected scan step was 0.6μm for general microstructure characterization and unit size measurements. The total scanned area was about 200×200μm^2. The criteria of 4º and 15º crystallographic misorientation boundaries were selected to quantify the mean grain sizes (Dmean-4º and Dmean-15º) and the corresponding size distributions. The effective grain size was calculated as the equivalent circle diameter related to the individual grain area. The 4º misorientation was selected as these boundaries intervene in the definition of yield strength, while the 15º boundaries are relevant to control brittle crack propagation (toughness).

Table 1 Chemical composition and mechanical properties of studied industrial samples

	Steel Grade	Sample	Thick/mm	C	Si	Mn	V	Nb	Reh/MPa	TS/MPa	A/%
Low Nb	QSTE340TM	C01	2.0	0.05	0.04	0.69	—	0.013	420	480	28.5
		C04	2.5						415	455	29.5
Low Nb Medium V	SAPH440	C05	4.0	0.06	0.03	0.75	0.031	0.013	415	480	37.5
		C06	5.0						420	480	36.0
Low Nb High V	QSTE380TM	C07	2.5	0.04	0.04	0.91	0.050	0.015	475	525	25.5
	QSTE420TM-B	C12	2.0	0.06	0.04	0.91	0.049	0.015	485	530	27.0
Medium Nb High V	QSTE500TM	C14	2.5	0.065	0.21	1.38	0.045	0.026	520	570	28.0
		C19	3.0						520	585	32.5
		C20	4.0						510	585	30.0
		C21	5.0						510	580	27.5

The industrial rolling schedules were analyzed with the help of MicroSim-DSP® (Direct Strip Processing) model version. The model predicts the austenite grain size distributions for recrystallized and unrecrystallized fractions at the entrance of any rolling pass, considering the metallurgical features acting during the interpass time. The model analyzes the complete austenite grain size distribution from pass to pass and it supplies the following data [3]:

(1) Recrystallized fraction.

(2) Non-recrystallized fraction detailing if the origin is solute drag or strain induced precipitation.

(3) Mean austenite grain size (Dmean).

(4) Critical grain size, Dc(0.1). This parameter corresponds to the grain size relative to the 10% of the coarsest grains in the tail of the distribution.

(5) Maximum austenite grain size (Dmax).

(6) ZD, the Dmax/Dmean ratio.

(7) The retained strain.

The application of the model to a specific industrial plant results in a valuable tool in the alloy/process design but it can require some level of customization. In this preliminary step to the application of the model, some specific characteristics of the production line, no implemented in the general version, are evaluated and included in the software.

2 Microstructural Characterization and Mechanical Behavior

Fig. 1 is an example of the EBSD analysis performed to characterize the industrial samples. In the figure, the image quality, the Inverse Pole Figure and the misorientation angle maps are reported. The grain boundary maps include the low (D-4º) and high (D-15º) angle crystallographic misorientation units represented in red and black, respectively. In this case, it is possible to observe a finer and more homogeneous microstructure when Nb content increases from 0.013% to 0.026%.

In addition to the mean unit size for both low (Dmean-4º) and high (Dmean-15º) angle crystallographic misorientations, the complete grain size distributions were determined. Fig. 2 shows the results obtained with sheets of 2.5 mm thickness and different Nb contents. They confirm the positive effect of Nb microalloying in the refinement of both low and high angle misorientation crystallographic units.

Once the microstructural characterization was done, it was possible to evaluate the role of different features on the mechanical behavior of the steels. For that purpose, the theoretical yield strength (σ_y) and tensile strength (UTS) are calculated based on the following

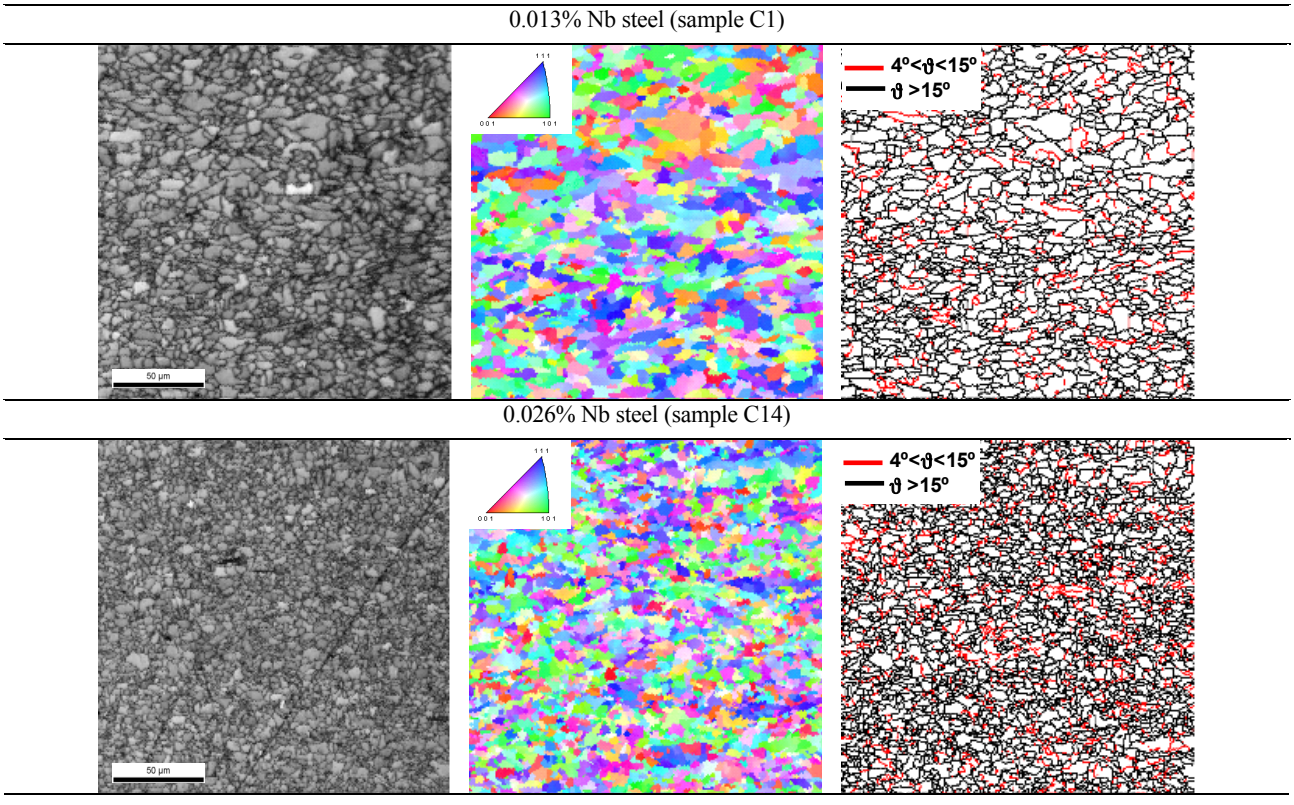

Fig. 1 Image quality maps, IPF (Inverse Pole Figure) and grain boundary maps (red lines > 4°, black lines > 15°) of two coils with different Nb amounts

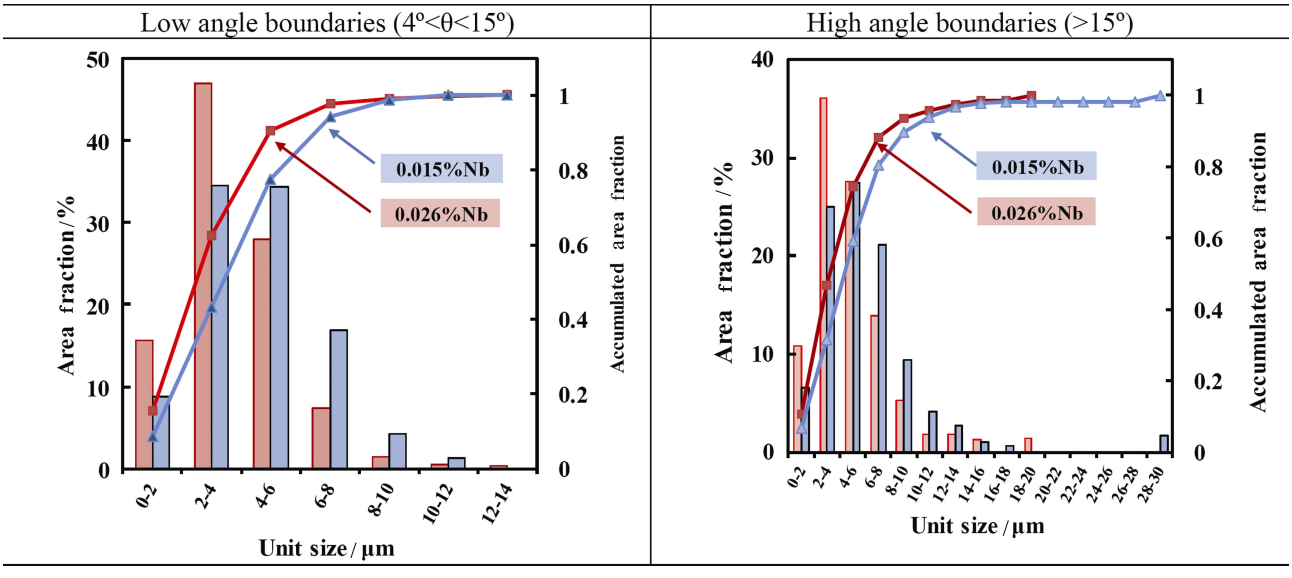

Fig.2 Grain size distributions (low and high angle boundaries) as a function of Nb addition (2.5 mm thickness)

equations proposed by Pickering [4]:

$$\sigma_y(\text{MPa}) = 53.9 + 32.3(\%\text{Mn}) + 83.2(\%\text{Si}) + 354(\%N_{free})^{0.5} + 17.4\,d_\alpha^{-0.5} \quad (1)$$

$$UTS(\text{MPa}) = 294 + 27.7(\%\text{Mn}) + 83.2(\%\text{Si}) + 678(\%\text{P}) + 3.85(\%\,pearlite)^{0.5} + 7.7\,d_\alpha^{-0.5} \quad (2)$$

where d_α is the ferrite grain size in mm (the 4º criterion has been considered) and N_{free} represents the free nitrogen content. As in this expression the contribution of precipitation and dislocation density is not considered (it was obtained for plain C-Mn ferritic microstructures), it is assumed that the differences between the real measurements and this theoretical prediction are due to this term: $\Delta\sigma_y = (\sigma_y)\text{measured} - (\sigma_y)$

predicted.

In this particular case, the contribution of free nitrogen is not quantified. As a consequence, the term $\Delta\sigma_y$ corresponds to the contributions of precipitation, dislocation density and free nitrogen. In relation to the UTS, the amount of pearlite has been assumed to be that corresponding to the equilibrium diagram.

The results obtained with each steel grade are illustrated in Fig. 3. Concerning the yield strength, the relevant role of grain size refinement is clearly identified in the figure. Depending on the microalloying addition and rolling strategy to aconditionate the austenite microstructure prior to transformation, the term associated with the grain size contribution goes from 256 to 348 MPa. That is, it can represent between 61% and 68% of the total strength of the steel.

In relation to the tensile strength, it is important to observe that in the empirical expression the "free nitrogen" contribution is not considered, as it happened with the yield strength. In consequence, the contribution of ΔUTS (the difference between the real measurements and those predicted by the previous equation), should be due mainly to precipitation strengthening.

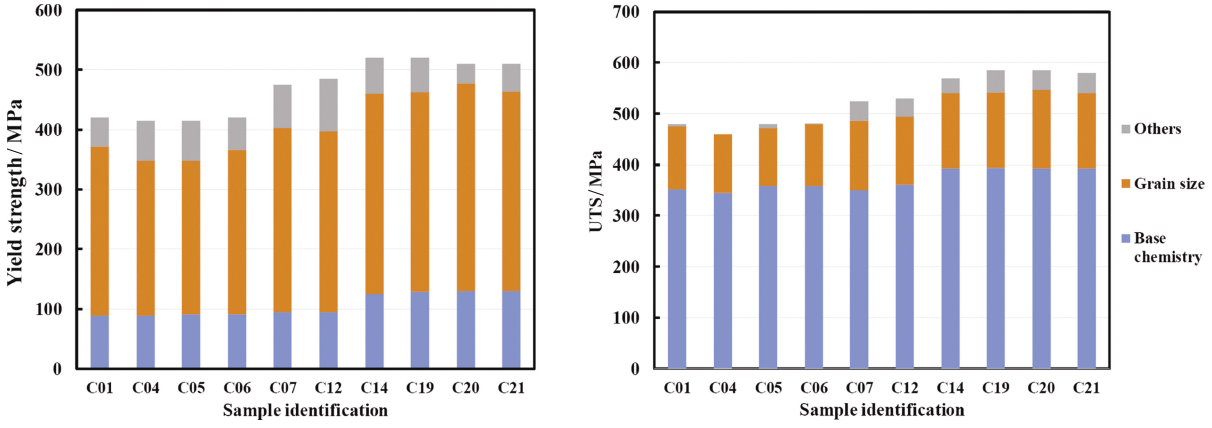

Fig. 3 Estimation of the contribution of each term to the yield and tensile strength

3 Application of MicroSim-DSP®

As mentioned before, in these steel grades the contribution of grain size refinement to the yield strength is very relevant. In addition, a fine and homogeneous microstructure exerts a relevant role in both ductility and toughness. Based on that, the refinement of the as-cast microstructure followed by a proper austenite conditioning prior to transformation becomes a key step in the industrial processing of the sheet. The application of MicroSim-DSP® model can help in the achievement of these objectives.

MicroSim model has implemented a procedure to perform a mechanical validation of its microstructural predictions. This is based on the calculation of the Mean Flow Stress (MFS) of each rolling pass and its comparison with real data collected from the rolling mill (the industrial MFS values are calculated based on the Sims method [5]).

In the industrial case of Handan, the TSCR process is characterized by the application of important reductions in the R1 roughing stand at relatively high temperatures. This combination of strain and temperature favors the activation of dynamic recrystallization that it is no so relevant in other TSCR configurations. This has been taken into account in the model predictions (microstructure and MFS values).

Fig. 4 shows the comparison between real and predicted MFS values for the low Nb grade (0.013%Nb, steel C04) as a function of inverse absolute temperature. If recrystallization occurs from pass by pass, a linear relationship exists between MFS and the inverse absolute temperature, $1/T$[5]. This is the behavior observed between R1 and F3 passes. In contrast, an increase and deviation in the MFS value occurs if strain accumulates (uncompleted recrystallization during the interpass interval). This can occur due to solute drag effect or Nb(C,N) strain induced precipitation. In the case of Fig.4, the change in the slope of MFS is denoting an important pancaking of austenite microstructure in F4~F6 passes. In the figure, the values of the Recrystallization Limit Temperature

(RLT, the lowest temperature above which recrystallization between passes is at least 80%) and the non-recrystallization temperatures (T_{nr}, temperature below which complete static recrystallization does not occur during the interpass time) are detailed, both provided by MicroSim predictions.

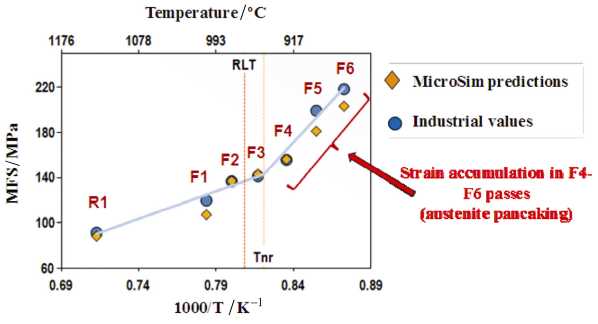

Fig. 4 MFS values obtained from mill loads and those predicted by the model in the case of 0.013%Nb steel

The MicroSim predictions concerning the evolution of the recrystallized fraction from pass to pass can be drawn as a function of the inverse absolute temperature, as shown in the scheme of Fig. 5. In the figure, three regions delimited by the recrystallization limit (RLT) and recrystallization stop (RST) temperatures, can be defined. RST represents the highest temperature at which recrystallization is completely absent and strain is accumulated. These two temperatures define three possible regions concerning austenite evolution [6]. In the region above RLT, defined as Type Ⅰ, complete recrystallization happens. Below RST, Type Ⅱ occurs, which implies strain accumulation and austenite pancaking. Finally, the interval between RLT and RST temperatures, defined as Type Ⅲ, corresponds to a situation of mixed austenite with recrystallized and deformed grains. When high mechanical properties are required, a proper amount of deformation in the Type Ⅰ and Type Ⅱ recrystallization regions should be targeted in the alloy/process design, while deformation in the Type Ⅲ recrystallization region should be minimized [7].

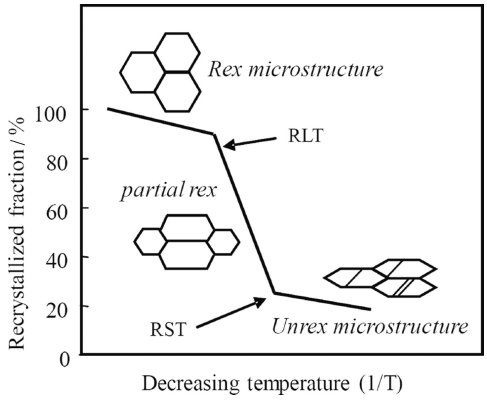

Fig. 5 Microstructural regions in relation to the evolution of the recrystallized fraction with temperature

Fig. 6 corresponds to the evolution of the recrystallized fraction for two conditions. As observed, in the case of Fig. 6(b), the higher amount of Nb allows to a better achievement of a proper Type Ⅱ austenite microstructure, while in the case of Fig. 6(a), the lower room temperature mechanical requirements could be obtained with a combination of recrystallized and non-recrystallized austenite grains.

Finally, the model allows analyzing the evolution of the austenite grain size distribution from pass to pass, as shown in the example of Fig. 7. In addition to the grain size refinement observed from pass to pass, the different contributions of recrystallization, non-recrystallization due to solute drag or to Nb(C,N) strain induced precipitation are indicated. In this case, the model predicts that, before transformation, the fraction of pancaked austenite is mainly due to strain induced precipitation, with a small relevance of solute drag.

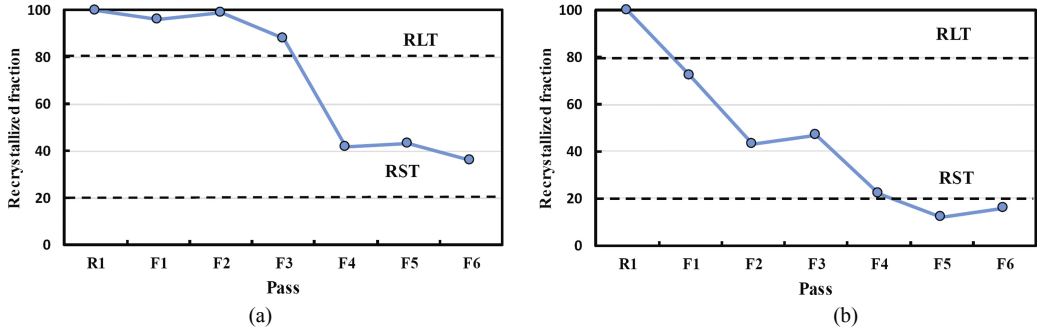

Fig. 6 Recrystallized fraction predictions for (a) 0.013%Nb (2. 5 mm thickness, C04) and (b) 0.026%Nb (4.0 mm thickness, C20)

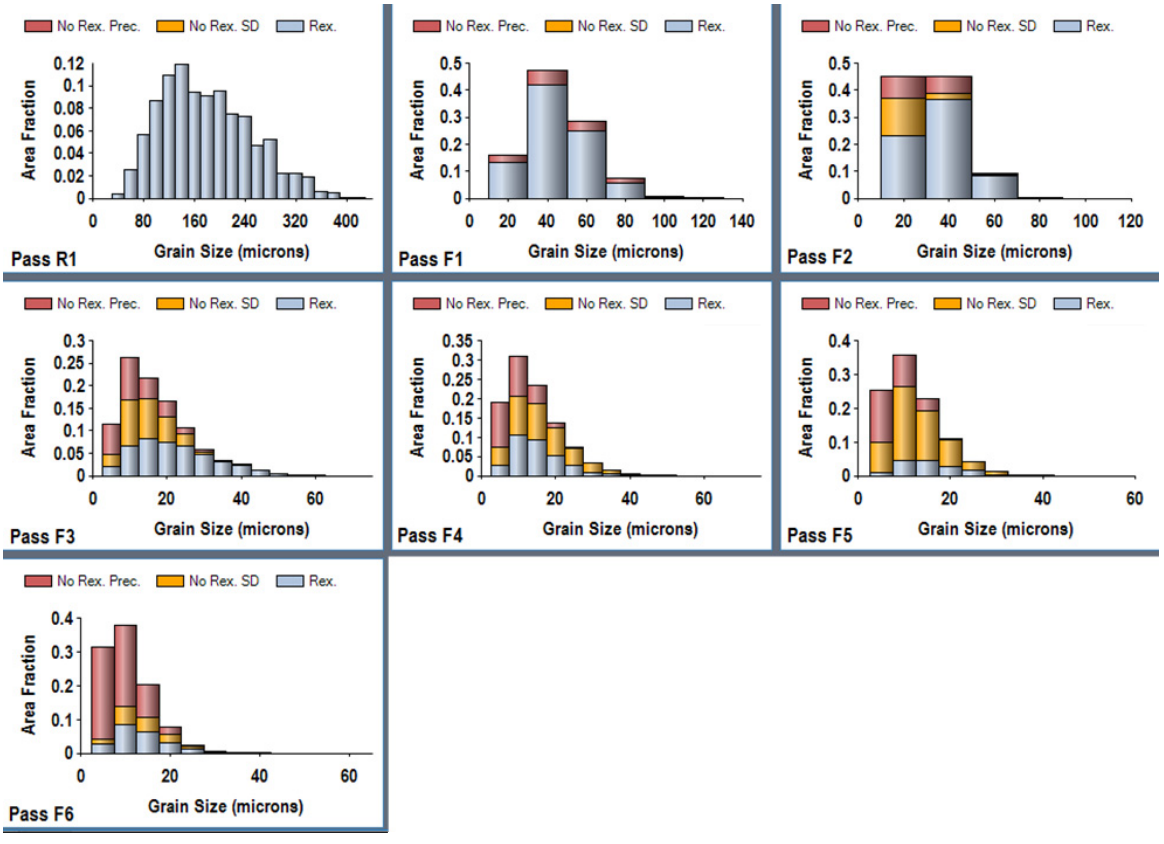

Fig. 7 Evolution of austenite microstructure predicted by MicroSim for the case of sheet C14

Depending of the final sheet thickness, the rolling strategy will change and this can affect the nature of final austenite microstructure. Fig. 8 is an example of this situation. It corresponds to the predictions obtained with MicroSim model for the case of QSTE500TM grade and final gauge thicknesses ranging from 2.5 to 5 mm with the same heat chemistry. It is possible to identify the different roles of solute drag and strain induced precipitation in the pancake austenite prior to transformation. Depending on the cooling and coiling strategies, these features can led to different refinements of the final microstructure. In consequence, depending of the mechanical requirements, the model can help to optimize the chemistry/process parameters required for each situation. This can be done with a combination of cost-effective solution.

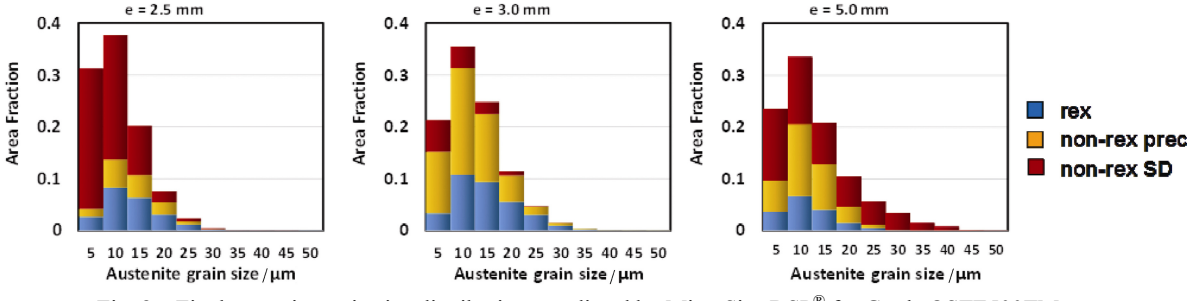

Fig. 8 Final austenite grain size distributions predicted by MicroSim-DSP® for Grade QSTE500TM as a function of final gauge thickness

4 Conclusions

This paper has evaluated the possibilities that can be achieved in practical industrial conditions combining microstructural analysis with MicroSim-DSP® software predictions. This has been applied to Handan Steel production of HSLA based Nb steel grades. With the help of the model, a complete understanding of the

effect of schedule parameters and compositional changes on the austenite evolution during thermomechanical processing can be achieved. In addition, this approach allows having a very useful information concerning final microstructural homogeneity. Based on this, it is possible to define different chemistry/process strategies that could also consider the definition of a cost-effective solution for each specific final application.

Acknowledgements

The authors would like to gratefully acknowledge HBIS-Handan Iron & Steel Group Co., Ltd. for permission to publish this paper and Companhia Brasileira de Metalurgia e Mineração (CBMM) for funding this project.

References:

[1] Uranga P, Fernández A I, López B, et al. Modeling of Austenite Grain Size Distribution in Nb Microalloyed Steels Processed by Thin Slab Casting and Direct Rolling (TSDR) Route, ISIJ Int, 2004, 44(8):1416~1425.

[2] Uranga P, Isasti N, Rodriguez Ibabe J M, et al. Optimized Cost Effective Production of Structural Hot Rolled CSP Coils through Proper Austenite Conditioning, Proc. AISTech 2017, Nashville, USA, 2975~2987.

[3] Pereda B, Uranga P, López B, et al. Mill Data based Microstructural Modelling for Thin Slab Direct Rolling of Nb Microalloyed Steels, Proc. 4th Int. Conf. on Thermo-mechanical Simulation and Processing of Steels, SimPro '16, 2016, Ranchi, India, 196~206.

[4] Pickering F B. Physical Metallurgy and the Design of Steels, London: Applied Science Pub., 1978, p. 37.

[5] Jonas J J. The Hot Strip Mill as an Experimental Tool, ISIJ Int., 2000, 40: 731~738.

[6] Samuel F H, Barbosa R, Boratto F, et al. Laboratory Simulation of Flow Stresses during Strip Rolling using High Strain Rate Torsion Testing, Thermec´88, Iron and steel Institute of Japan, 1988, 2: 721~728.

[7] Kendrick V, Frye B, Sutcliffe A, et al. Evaluation of Toughness Characteristics of API Grade Pipeline Steel Produced on Compact Strip Production (CSP) Line, 11th Intern. Pipeline Conf. IPC2016, ASME, 2016, IPC2016-64153.